Bursting and mixed mode oscillations during the transition to limit cycle oscillations in a matrix burner

Praveen Kasthuri, Vishnu R. Unni, and R. I. Sujith

View Online   Export Citation   CrossMark

ARTICLES YOU MAY BE INTERESTED IN

AIP Author Services
English Language Editing

Bursting and mixed mode oscillations during the transition to limit cycle oscillations in a matrix burner

View Online   Export Citation   CrossMark

Praveen Kasthuri,[1,a)] Vishnu R. Unni,[2] and R. I. Sujith[1,b)]

AFFILIATIONS

[1] Department of Aerospace Engineering, Indian Institute of Technology Madras, Chennai 600036, India
[2] Department of Mechanical and Aerospace Engineering, University of California San Diego, 9500 Gilman Dr., La Jolla, California 92093, USA

[a)] **Electronic mail:** kpn1994@gmail.com
[b)] **Also at:** Department of Aerospace Engineering, Indian Institute of Technology Madras, Chennai 600036, India.

ABSTRACT

We investigate the route to self-excited thermoacoustic instability in a laminar flow multiple flame matrix burner. With an increase in the equivalence ratio, the thermoacoustic system that is initially quiet (stable operation) transitions to limit cycle oscillations through two distinct dynamical states, namely, bursting oscillations and mixed mode oscillations. The acoustic pressure oscillations transition from quiescence to large amplitudes during bursting oscillations. Such high amplitude bursting oscillations that occur well ahead of the onset of limit cycle oscillations can potentially cause structural damage. The thermoacoustic system exhibits hysteresis. The transition to limit cycle oscillations is replicated in a phenomenological model containing slow-fast time scales.

Published under license by AIP Publishing. https://doi.org/10.1063/1.5095401

Confined combustion systems are often susceptible to large amplitude pressure oscillations, otherwise known as thermoacoustic instability. Thermoacoustic instability results from the coupled interaction between the acoustic field and heat release rate oscillations in the combustor. Thermoacoustic instability exposes rocket and gas turbine engines to increased heat transfer that can overwhelm the thermal protection mechanisms and affect the onboard navigation system, electronics, payload, and even lead to mission failure. It is important to characterize the route from stable operation to thermoacoustic instability. Further, a comprehensive understanding of all possible dynamics is necessary to design appropriate control measures to mitigate thermoacoustic instabilities and to operate the combustor safely in a wider envelope. Route to thermoacoustic instability can vary according to combustor configuration and operating conditions. Here, we discuss the route from stable operation to thermoacoustic instability in a multiple flame combustor. We see that a multiple flame combustor transitions to limit cycle oscillations via a route not reported before, characterized by the occurrence of bursting and mixed mode oscillations.

I. INTRODUCTION

Thermoacoustic instability is a crippling issue in the development and safe operation of thrust-producing devices such as liquid and solid rocket motors, aero-engines, and in power-producing machines such as land based gas turbine engines.[1,2] This phenomenon is a consequence of the positive feedback between the acoustic pressure oscillations in the combustion chamber and the heat release rate fluctuations of the flame.[3] The violent periodic oscillations generated from the occurrence of thermoacoustic instability could drastically reduce the lifespan of engine components and possibly lead to partial or total mission failure in the case of rocket motors.[4–6] The severity of the devastating effects of thermoacoustic instability gained attention with humongous amount of funds spent on thousands of full-scale tests to mitigate such instabilities faced in the F-1 rockets.[7] Subsequently, there have been many rockets, aero-engines, and power-producing gas turbines which faced these issues. Ever since, a plethora of researchers have focused on characterizing the behavior of combustors during thermoacoustic instability and suppress instability using several *ad hoc* control strategies.

However, it is vital to understand how a combustion system transitions from stable operation to thermoacoustic instability in order to prognose the onset of thermoacoustic instability and devise control mechanisms necessary to mitigate thermoacoustic instability.

Existing literature points out that systems operating under laminar and turbulent flows approach thermoacoustic limit cycle oscillations (LCOs) via different routes. For a horizontal Rijke tube under laminar flow conditions, with a heated wire mesh as the source of heat, the transition from stable operation to limit cycle oscillations occurs either through a subcritical or supercritical Hopf bifurcation[8–10] depending on the flow rates of the working fluid. In a Rijke tube with a premixed laminar flame as the heat source, Weng et al.[11] reported the presence of beats characterized by amplitude modulated periodic oscillations en route to LCO.

Dynamically, the transition to thermoacoustic instability in laminar systems is viewed as a transition from a fixed point to limit cycle oscillations. However, in turbulent systems, the stable state cannot be considered as a mere fixed point. The stable operation, also known as combustion noise, is characterized by aperiodic oscillations. Such aperiodic oscillations are attributed to the background turbulence and are reported to contain features of high-dimensional chaos contaminated with noise.[12] On the other hand, unstable operation, in general, is composed of large amplitude periodic oscillations and is popularly known as thermoacoustic instability. Thus, the transition to thermoacoustic instability in turbulent systems should be viewed as an emergence of order (periodicity) from chaos.[13]

Gotoda et al.[14] showed that the dynamics of a premixed gas turbine combustor transitions from the state of combustion noise to periodic oscillations through low dimensional chaotic oscillations with an increase in the equivalence ratio. Thereafter, Nair et al.[15] showed that the transition from stable state to thermoacoustic instability occurs via intermittency in a turbulent combustor. They referred to intermittency as an asymptotic state characterized by the apparently random occurrence of bursts of periodic oscillations amidst epochs of aperiodic oscillations. Since then, intermittency has been observed in various liquid and gaseous fuel combustors despite the differences in the flame stabilization mechanisms.[16–21] Recently, intermittency has also been discovered in the heat release rate dynamics of a composite propellant.[22] The occurrence of intermittency in turbulent thermoacoustic systems has been exploited to develop precursors to predict the onset of thermoacoustic oscillations.[23–25]

There have been studies that investigated the origin of intermittency. Pawar et al.[26] analyzed the coupled behavior between acoustics and reacting flow subsystems using synchronization theory. They showed that intermittency corresponds to intermittent partial synchronization of acoustic and heat release rate. Further, thermoacoustic instability is shown to be either a phase synchronized state or a generalized synchronization state. Mondal et al.[13] performed spatiotemporal analysis on the coupled interaction between acoustics and heat release rate. They viewed the transition as an emergence of order from disorder through a chimera-like state observed during intermittency wherein there is a simultaneous existence of regions of disorder and order in the reaction zone. Analyzing the flame dynamics during intermittency, Nair and Sujith[27] showed that the flame is intermittently detached from the flame-holder, thereby reducing the driving in the system. In a similar study, Unni and Sujith[28] found that

during intermittency, the flame exhibits two marked patterns of oscillations. The flame is oscillating either in an aperiodic manner due to the underlying turbulence or exhibits a periodic roll-up as a result of the periodic vortex shedding from the location where the flame is attached. In short, during the onset of thermoacoustic instability, laminar systems transit directly from fixed point to limit cycle oscillations and turbulent systems transition from chaotic oscillations to limit cycle oscillations via intermittency.

Recent studies have shown that post the onset of limit cycle oscillations, upon further variation of the corresponding parameter, thermoacoustic systems can exhibit other complex dynamical behaviors. Kabiraj et al.[29] showed quasiperiodic, frequency locked, period-2 and chaotic oscillations in addition to limit cycle oscillations during thermoacoustic instability. Kashinath et al.[30] examined the dynamics during the transition to and during thermoacoustic instability with numerical simulations of a coupled flame and acoustics model. They concluded that the nonlinear heat release rate simultaneously affects several acoustic modes leading to flame wrinkling through nonharmonic velocity perturbations. Their findings were in agreement with the experimental observations of Vishnu et al.[31] Recently, Guan et al.[32] showed the occurrence of period-2 and period-3 oscillations in an alternative manner in a composite propellant solid rocket motor. A bifurcation analysis performed on a thermoacoustic engine[33] showed that limit cycle oscillations in the fundamental mode are followed by quasiperiodic and other higher harmonic modes. An interesting study[34] performed on a premixed flame inside a duct under turbulent flow conditions showed beat oscillations composed of two beat frequencies and the harmonic of one of the beat frequencies during thermoacoustic instability. These beats are reported to be self-sustained by satisfying the Rayleigh criterion over a cycle of the oscillation even though the instantaneous phase condition within a cycle is not satisfied according to the Rayleigh criterion.[3]

In stark contrast to all these transition scenarios, we observe a novel route to thermoacoustic instability in a matrix burner with several interacting flamelets with a variation in the control parameter. We observe bursting oscillations[35–37] featured by the alternating occurrence of epochs of large amplitude periodic oscillations followed by quiescence during the transition from stable operation to thermoacoustic instability. Unlike the case of intermittency in turbulent systems, where the low amplitude fluctuations are aperiodic and have deterministic nature, the quiescent epochs during bursting oscillations are devoid of any perceivable deterministic signature. During thermoacoustic instability, we detect mixed mode oscillations (MMOs) characterized by periodic oscillations switching between mostly two amplitudes prior to attaining limit cycle oscillations. We show that bursting and mixed mode oscillations are the result of interaction between the slow and fast time scales in the system.

Bursting has been observed in several systems ranging from neuronal activities,[37,38] electrochemical reactions[39] to medicine.[40] Knobloch and Koehlis[41] reviewed several mechanisms for bursting behavior in hydrodynamic systems. One possible mechanism for bursts in the event of a Hopf bifurcation from the base state for systems with a broken D_4 symmetry (symmetry group of a square geometry) was discussed. The nonlinear interaction between the different broken symmetries in the system generate bursts.

The bursts occurring in shear flows undergoing subcritical transition to turbulence arise out of a different mechanism. The turbulence excited by the finite amplitude perturbations in shear flows often take the form of turbulent spots which can move, split, and merge. These turbulent spots exhibit bursts intermittently. Another mechanism for bursts pertains to coherent vortices evolving to a spatially disordered state following the transfer of energy from large to smaller scales.

There have been descriptions of dynamical behaviors in thermoacoustic engines that fit the description of bursting oscillations. A thermoacoustic engine is another popular system composed of a working gas flowing through a porous stack placed between the hot and cold heat exchangers.[42] Unlike the thermoacoustic systems discussed so far, the mechanism of acoustic power generation is different in thermoacoustic engines. In a thermoacoustic engine, the high amplitude pressure oscillations arise due to the temperature gradient established across the stack. A study performed on a traveling wave thermoacoustic engine, Lawn and Penelet,[42] and Wu *et al.*[43] showed a periodic process of onset-quenching of oscillations across a range of heater power prior to sustained LCOs. The pressure oscillations grow from small to large amplitudes during the onset process and drops quickly with a sharp decay rate during the quenching process. The periodic process of onset-quenching starts with the onset at a high frequency mode, to quenching with a low frequency mode. This onset-quenching of oscillations terminates with a sustained LCO at a low frequency mode.

Some studies have reported bursts of oscillations while characterizing the behavior of thermoacoustic engines. For example, Lawn and Penelet[42] and Abduljalil *et al.*[44] reported that during the nonlinear startup process in a looped tube thermoacoustic engine, different transient phenomena such as the "on-off effect" and "fishbone-like" bursts are observed for varying mean pressure and input heat power. However, studies reporting bursts of oscillations do not necessarily refer to the bursting oscillations described in our study. Similarly, bursting oscillations are different from beats wherein there exists a periodic amplitude modulation over the underlying periodic oscillations. In contrast, bursting oscillations are composed of regions of sustained periodic oscillations interspersed between regions of quiescence, as observed in our system.

The paper is outlined as follows: In Sec. II, we describe the experimental setup used in this study. In Sec. III, the transition from stable operation to thermoacoustic instability is characterized, emphasizing the bursting and the mixed mode oscillations. We follow up with a bifurcation analysis and conclude this section by presenting a low-order model replicating the features observed in the experiment. Finally, we summarize the findings in Sec. IV.

II. EXPERIMENTAL SETUP

Experiments are performed on a laboratory scale premixed matrix burner housing multiple injectors. The flow through the injectors is in the laminar flow regime. Many practical applications such as rocket engines, modern gas turbine engines, smelters, etc. involve the interaction of multiple flames across its burners. With the intention of characterizing the dynamical behavior in the presence of multiple flames, we built this matrix burner containing many interacting flamelets. A schematic of the experimental setup with a zoomed-in illustration of the burner is shown in Fig. 1. The setup consists of a

premixer, a settling chamber, and a burner, which is confined within a quartz duct of 80 cm length and 5.5 cm diameter. The relative position of the burner within the quartz duct is fixed 38 cm upstream from the open end of the quartz duct. Dehumidified air supplied from a compressor is mixed with liquefied petroleum gas (LPG containing 60% butane and 40% propane) in a premixer stuffed with steel wool, prior to entering the settling chamber. The premixed reactants are transported from the settling chamber to the burner through a stainless steel tube of 19 mm diameter. The matrix burner consists of 112 injectors of diameter 1 mm each arranged in four concentric annuli with uniform spacing within each annulus. Through these injectors, the premixed mixture is issued to the reaction zone. Flame arrestors are placed at the exits of the settling chamber and the premixer for preventing flashback.

The flow rates of fuel and air are controlled using mass flow controllers (Alicat Scientific MCR series) with an uncertainty of $\pm(0.8\%$ of reading $+ 0.2\%$ of full scale). Unsteady pressure fluctuations are measured using a piezoelectric transducer (PCB103B02 with sensitivity of 217.5 mV/kPa) with an uncertainty of ± 0.15 Pa located on the quartz glass 38 cm upstream from the open end of the duct. A signal conditioner (PCB Piezotronics 482C05) operated at gain 1:1 is used to condition the signal from the pressure transducer. The equivalence ratio (ϕ), which is defined as the ratio of the actual fuel/air ratio to the stoichiometric fuel/air ratio, is varied between 0.341 ± 0.002 and 0.522 ± 0.003. The corresponding Reynolds number (Re), which compares the inertial forces to viscous forces, is varied in the range 1260–1916 with an uncertainty of ± 16. A K-type thermocouple is used to measure the temperature close to the burner. The signals from the pressure transducer are acquired using a 16 bit A/D card (NI-6343) at a sampling rate of 12 000 Hz. Simultaneously, the temperature data are acquired by another A/D card (Agilent-34970A) at a sampling rate of 20 Hz.

III. RESULTS

The primary objective is to study the route to thermoacoustic instability in a multiple flame burner. In order to do that, we vary the air flow rate from 27.6 SLPM to 18.0 SLPM in steps of 0.1 SLPM, maintaining the fuel flow rate fixed at 0.6 SLPM to alter the equivalence ratio and observe the changes in the dynamical behavior of the system. The whole range of air flow rates traversed translate to an equivalence ratio variation from 0.341 to 0.522. We characterize the dynamics of combustor by studying the temporal behavior of acoustic pressure oscillations.

A. Route from stable operation to limit cycle oscillations

As we vary the equivalence ratio, we encounter different dynamical behaviors in the combustor. In Fig. 2, we show the representative time series for each kind of dynamical behavior observed. For $\phi = 0.341$, the pressure oscillations [see the inset of Fig. 2(a)] correspond to a quiescent state with amplitudes comparable to the measurement noise floor (10 Pa). We refer to this state of the system as stable operation. When the equivalence ratio is increased, we observe bursts of periodic oscillations amongst quiescence, alternating in an apparently random manner [Fig. 2(b)]. This dynamical behavior is referred
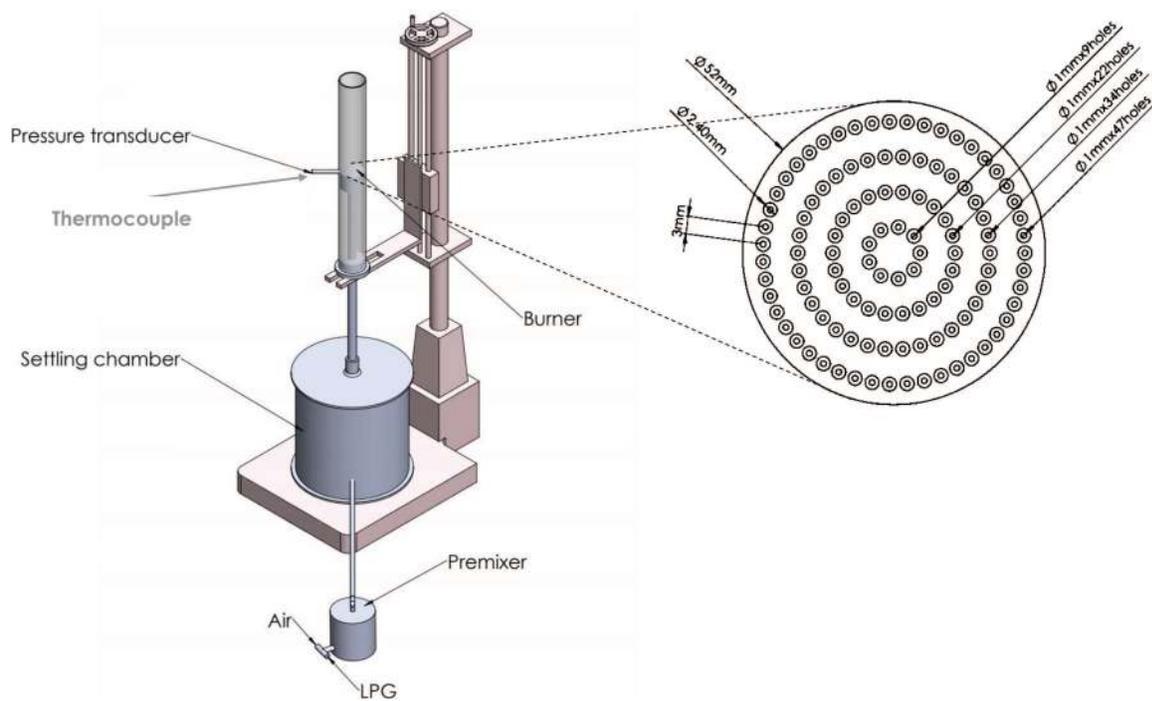
FIG. 1. Schematic of the multiple flame matrix burner with details of the burner geometry.

to as bursting oscillations, wherein the signatures of both the stable operation and unstable operation coexist.

Upon further increase of ϕ till 0.346, the seemingly random occurrences of these bursts are more frequent. From $\phi = 0.347$ to 0.522 in Figs. 2(c)–2(f), we observe that the entire time series of acoustic pressure is completely composed of periodic oscillations. However in Figs. 2(c)–2(e), the amplitude switches from one level to another. Such oscillations where periodic oscillations shift between two or more well determined amplitude levels (categorized as slow and fast amplitudes) are known as mixed mode oscillations (MMOs).[35,45] MMOs have been found in neuronal activites,[46] electro-chemical reactions,[39,47,48] climate models[49] to plasma instabilities.[50]

With further increase in ϕ till 0.392 [Figs. 2(c)–2(e)], the switching between high and low amplitudes increases until the oscillations transform to the high amplitude limit cycle (amplitude of around 440 Pa). This high amplitude limit cycle persists until ϕ reaches 0.522. This gradual transition from MMOs to a high amplitude limit cycle with an increase in ϕ is apparent in Figs. 2(c)–2(f). In summary, the system that is initially stable transitions to limit cycle oscillations through two distinct states, namely, bursting oscillations and mixed mode oscillations.

The spectral evolution of the dynamics of acoustic pressure oscillations for each dynamical state is shown in a spectrogram (first column) in Fig. 3. We observe that the stable operation does not contain any dominating frequency. We observe a range of frequencies during the large amplitude epochs of bursting oscillation and during mixed mode oscillations. Examining the spectrogram, we found that

the large amplitude portion of the mixed mode oscillation exhibits a slightly broader range of frequencies between 288 Hz and 370 Hz when compared to 278 Hz to 330 Hz for small amplitude oscillations. A similar change in the dominant frequencies during small and large amplitude oscillations are observed in their corresponding harmonics. We expect this difference in the frequencies to arise due to the different temperature profiles established in the combustor during large amplitude and small amplitude oscillations. During limit cycle oscillations, we note a sharp peak at 328 Hz and strong periodic content also in its harmonics. The dominant frequency calculated for the entire time series for each state is captured by the amplitude spectrum shown in the second column of Fig. 3.

The corresponding reconstructed phase spaces for the different states of combustor operation are portrayed in the third column of Fig. 3. We notice a cluster of points during stable operation with no discernable pattern to the phase space [Fig. 3(a)]. The phase space is a planar disk-like structure during bursting oscillations [Fig. 3(b)] superimposed with a similar clutter of points occupying the phase space volume close to zero amplitude. During mixed mode oscillations [Fig. 3(c)], we observe a similar disk-like structure. However, the clutter of points around zero amplitude is absent and the trajectory spirals between the low and high amplitude periodic orbits. Finally during limit cycle oscillations [Fig. 3(d)], we obtain a ring-like structure.

Several studies have attributed the nonlinear interaction of the multiple time scales to the occurrence of bursting oscillations and mixed mode oscillations.[35,45] In this study, throughout the transition
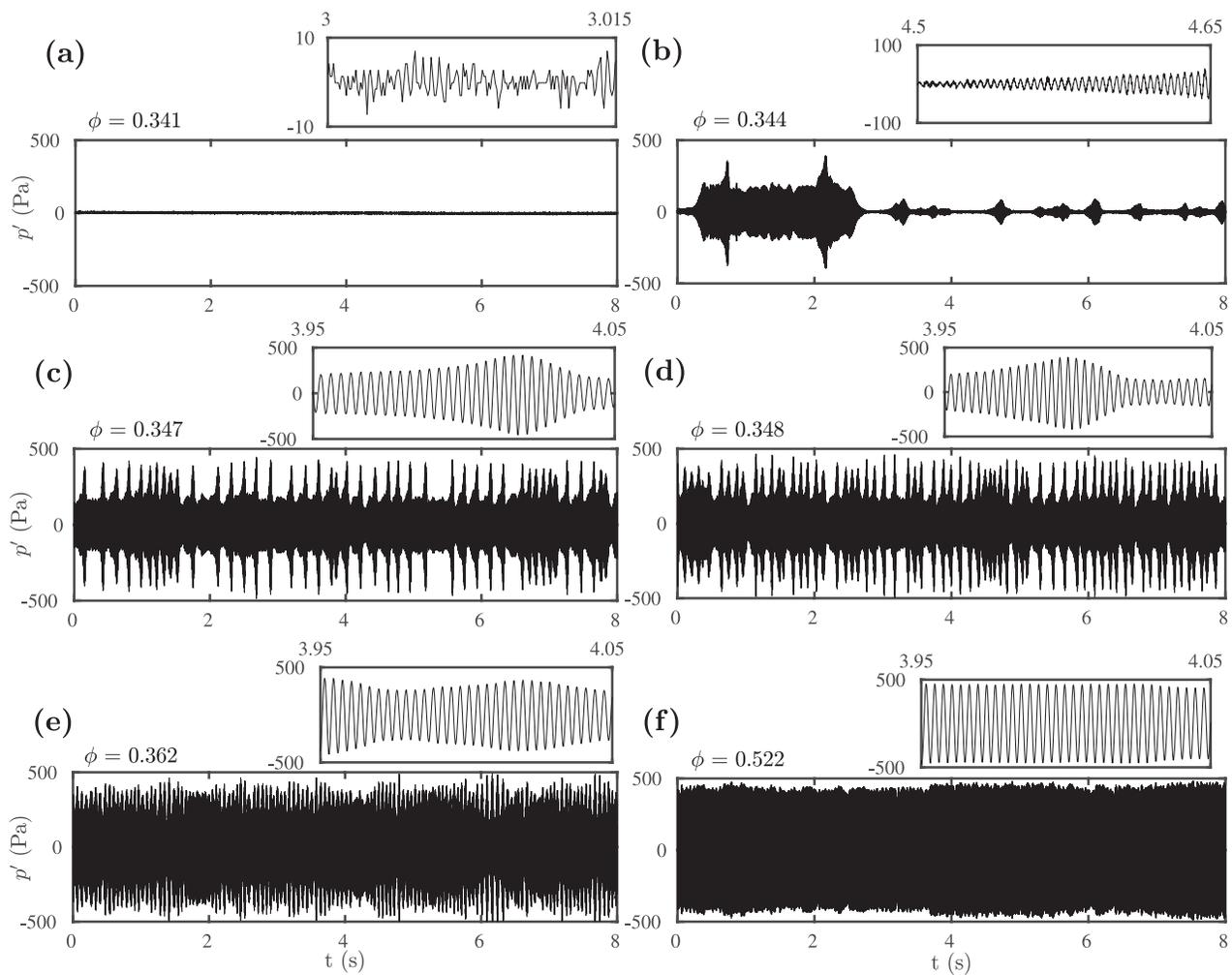
FIG. 2. Time series of acoustic pressure oscillations (p') inside the duct for different equivalence ratios (ϕ). (a) For $\phi = 0.341$, the system is at a stable state. (b) for $\phi = 0.344$, the system exhibits bursting oscillations, wherein epochs of periodic oscillations exist amongst the quiescence. (c)–(e) For the range $\phi = 0.347$ to 0.392, the acoustic pressure oscillations represent mixed mode oscillations. (f) With a further change in ϕ, a constant large amplitude limit cycle is established.

from stable operation to limit cycle oscillations, the individual flamelets stabilized above the matrix burner oscillate up and down within the confinement. This leads to a spatial and temporal variation in the heat release rate oscillations. The corresponding temporal behavior in the temperature is captured by a K-type thermocouple placed at the same location as the pressure measurement. The time series of acoustic pressure oscillations and the corresponding temperature oscillations during the state of bursting oscillations are shown in Figs. 4(a) and 4(b). We observe that whenever a burst of high amplitude oscillation arises out of quiescence, the temperature drops. The temperature rises again as soon as the burst of high amplitude oscillation starts to decay to quiescence. Additionally, we observe that with prolonged burst duration, the temperature keeps dropping to lower values until the oscillations become quiescent [see the region enclosed by a green rectangle around 50 s in Figs. 4(a) and 4(b)].

In summary, this analysis proves the simultaneous coexistence of the slow-fast time scales in the thermoacoustic system. Hence, we conjecture that the interplay between these two time scales leads to bursting oscillations and mixed mode oscillations in the system.

B. Bifurcation analysis

Next, we study the bifurcation characteristics of the system to unravel the hysteresis effects. A dedicated experiment for acquiring the acoustic pressure oscillations for finer steps of 0.1 SLPM in the volumetric air flow rate is conducted. The root mean square (*rms*) and global maximum of the oscillations are plotted against equivalence ratio, as shown in Fig. 5(a). We note that the values of both the p'_{rms} and p'_{max} are close to zero during stable operation. During bursting oscillations and mixed mode oscillations, we observe a rise in the
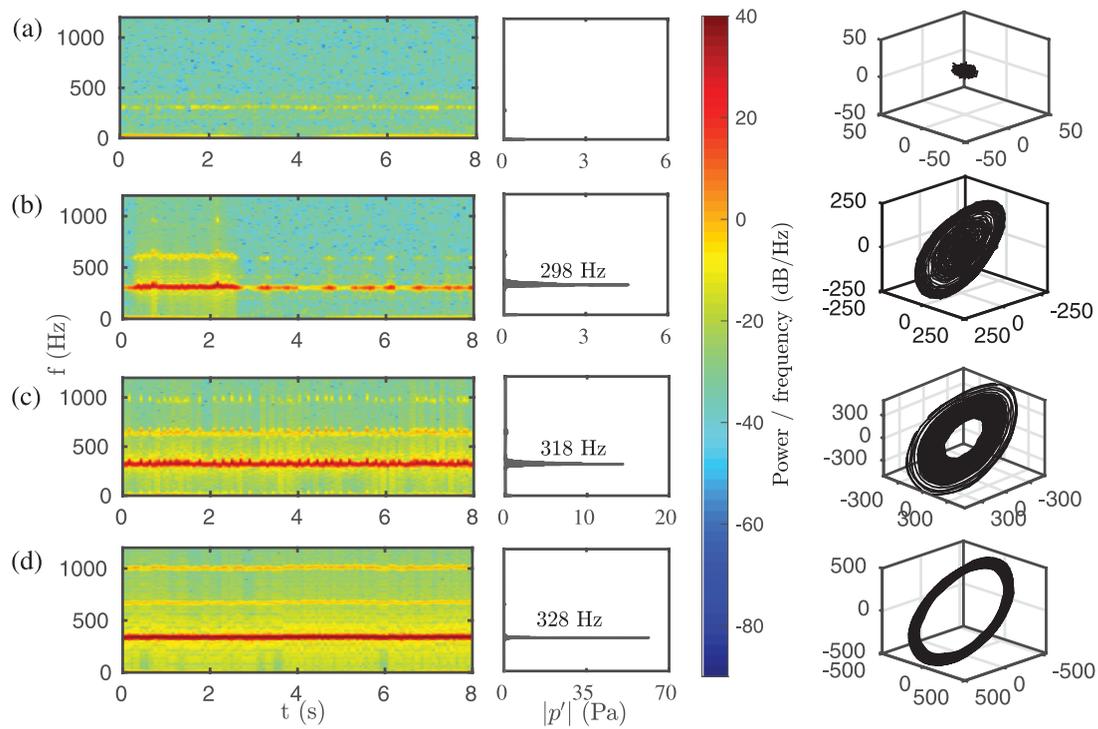
FIG. 3. Spectrogram showing the power spectrum of the frequencies against time calculated through FFT with a resolution of 2 Hz, amplitude spectrum calculated from FFT with a resolution of 1 Hz and the phase portraits are plotted in the first, second, and third columns for (a) stable operation, (b) bursting oscillations, (c) mixed mode oscillations, and (d) limit cycle oscillations, respectively. The spectrogram and the amplitude spectrum are labeled with the same ordinates. The dominating frequency is shown for each dynamical state in the corresponding amplitude spectrum.
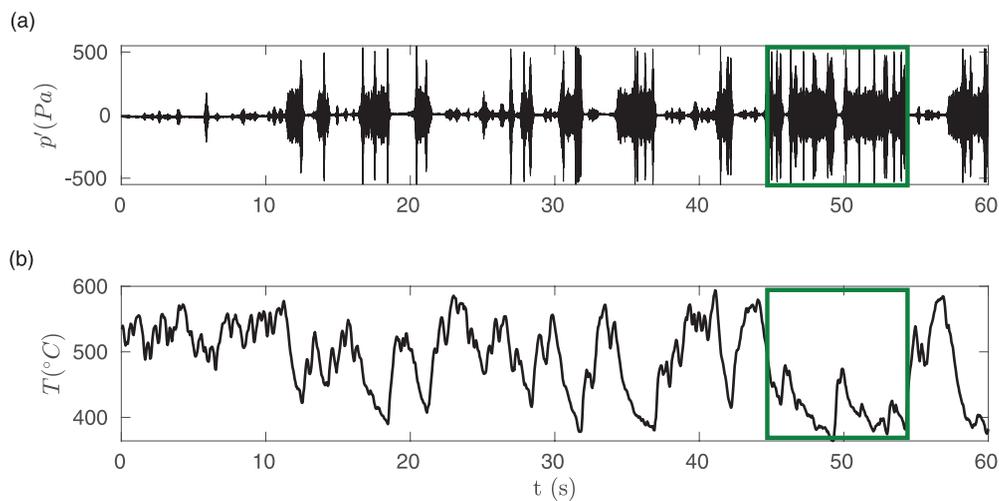

FIG. 4. The time series of (a) acoustic pressure oscillations and (b) temperature oscillations obtained simultaneously for a duration of 60 s during bursting oscillations. We conjecture that the simultaneous coexistence of slow-fast time scales gives birth to bursting and mixed mode oscillations.
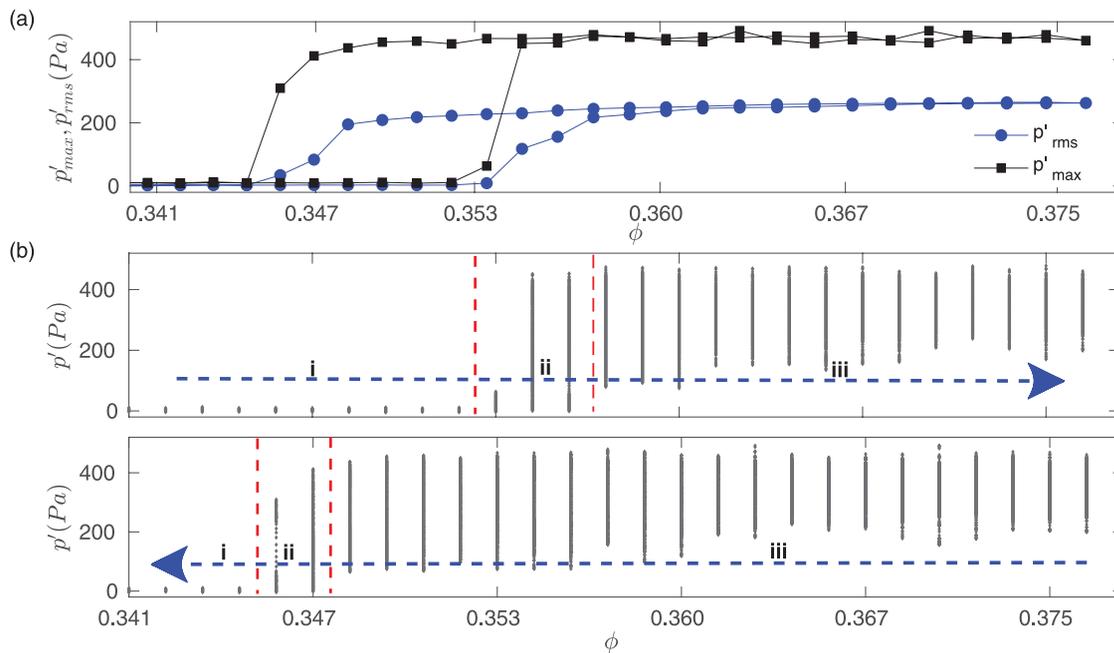
FIG. 5. (a) Root mean square and absolute maximum of the oscillations against equivalence ratio and (b) bifurcation plot for the local maxima of the acoustic pressure oscillations are sketched with equivalence ratio as parameter for both forward and reverse directions, as indicated by the blue dashed arrows. The red dashed lines divide the states of combustor operation: (i) stable operation, (ii) bursting oscillations, and (iii) mixed mode oscillations. We observe hysteresis in both the *rms* and the maximum of the acoustic pressure oscillations in both (a) and (b).

magnitudes of both p'_{rms} and p'_{max}. However, the value of p'_{max} is significantly higher than p'_{rms}, denoting that the combustor encounters oscillations having large instantaneous amplitudes well ahead of the occurrence of limit cycle oscillations. As the mixed mode oscillations transition to limit cycle oscillations, the magnitudes of p'_{rms} and p'_{max} saturate to their maxima of 260 Pa and 470 Pa, respectively.

In Fig. 5(b), a bifurcation plot tracking the various local maxima against ϕ for both the forward and reverse directions is shown. From Fig. 5(b), we observe that the minimum of the local maxima gradually increases with the equivalence ratio, while the maximum of the local maxima stays almost constant during mixed mode oscillations. A distinct hysteresis behavior is observed when the parameter is traversed in the reverse direction, as seen in Figs. 5(a) and 5(b). We note that the range of ϕ in the large amplitude portion is significantly higher in the reverse path. A characteristic feature observed in this system is that during bursting oscillations, the maximum of acoustic pressure oscillations (also for heat release rate oscillations) is close to the high values attained during large amplitude limit cycle oscillations. This behavior is in stark contrast compared to the behaviors seen in some turbulent combustors,[15,51] wherein the maximum instantaneous amplitude of the oscillations gradually increases from stable operation to thermoacoustic instability with intermediate values during intermittency. For a spray combustor, Pawar *et al.*[19] reported higher magnitude of oscillations during intermittency than during thermoacoustic instability. In this study, the magnitude of the oscillations attains the maximum value of 470 Pa during bursting oscillations itself. However, unlike the results for

this spray combustor,[19] the amplitude of oscillations during thermoacoustic instability is not lower than the maximum amplitude during bursting and mixed mode oscillations. The occurrence of high amplitude oscillations during bursting oscillations, if observed in practical scenarios could be disastrous as the combustor is exposed to large structural and thermal loads, well before the onset of thermoacoustic instability and could possibly lead to structural damage.

C. Model

A reduced order phenomenological model is constructed with the aim of capturing the dynamics observed in experiments. Similar models have been used to replicate other known dynamics of thermoacoustic systems.[52,53] Essentially, the model represents a self-excited nonlinear oscillator and it displays the different dynamical states during the transition observed in the experiment. Several studies[54–56] have showed the necessity of a slow time scale to obtain bursting and mixed mode oscillations. For simplicity, a slow time scale in the form of a low frequency periodic oscillation is used in addition to the inherent fast acoustic time scale. Further, this model can be shown to fit into the family of slow-fast equations as explained in Kuehn.[57]

The acoustic pressure (η) and the acoustic velocity ($\dot{\eta}$) are coupled through the set of governing equations shown in Eqs. (1)–(3). Equation (1) depicts the evolution of the nonlinear self-excited oscillator modeling the acoustic pressure (η) oscillating at its preferred frequency (ω). The driving and damping in the system are contained
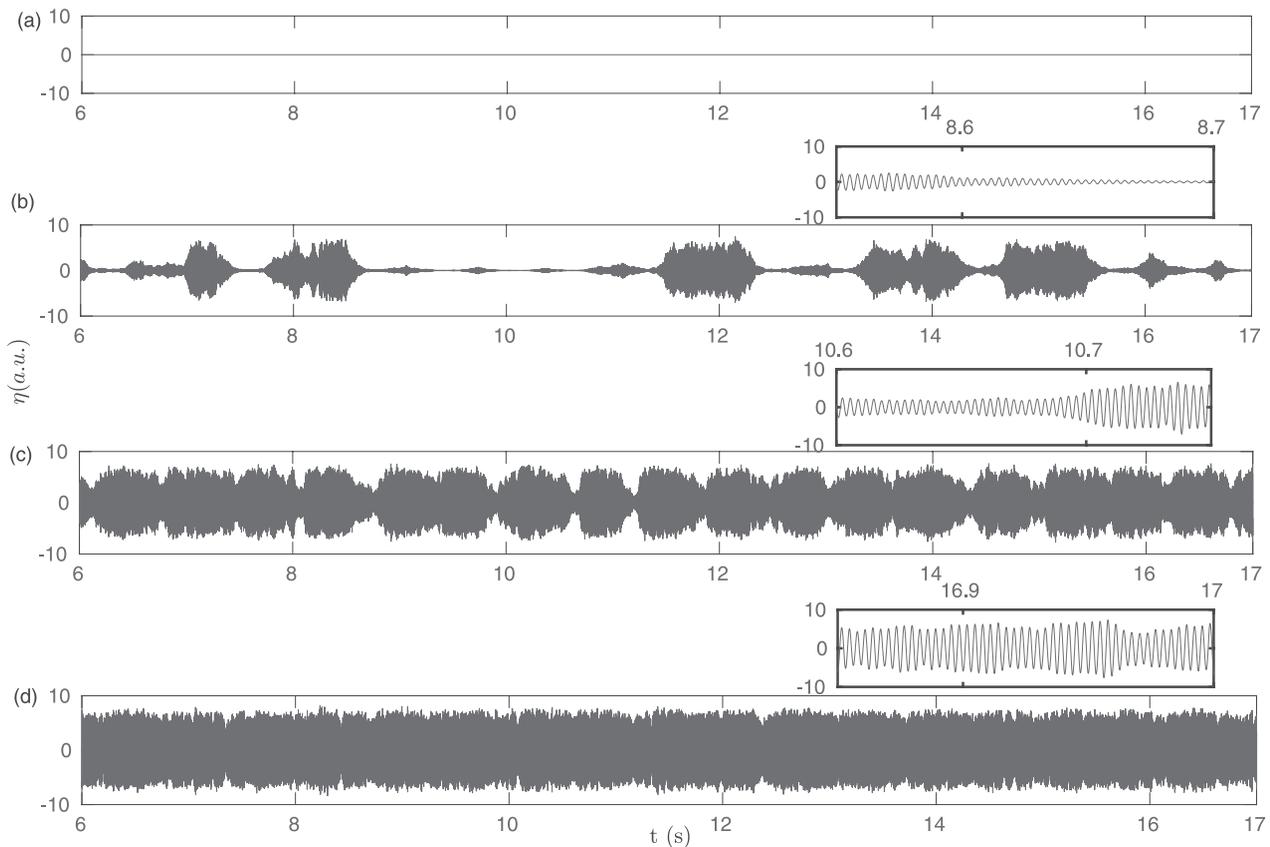
FIG. 6. The time series of acoustic pressure fluctuations along with their zoomed insets obtained using the model is shown during (a) stable operation, (b) bursting oscillations, (c) mixed mode oscillations, and (d) limit cycle oscillations. The values of $\alpha = 58, 52, 37,$ and 5 rad/s, respectively.

in $f(\eta, \dot{\eta})$ occurring in the right hand side of Eq. (1). A low frequency periodic oscillation of frequency (ω_q) with a coupling strength q_a is coupled to the acoustic velocity rather than to the acoustic pressure as shown in Eq. (2). This is because the slow phenomena such as hydrodynamics and heat transfer in a thermoacoustic system are influenced directly by the acoustic velocity.[1] The relation between the heat release rate term q_c and acoustic pressure is given by Eq. (3). The heat release rate oscillations are modeled as a fifth order polynomial in η. The coefficients α and β can be varied to alter the damping and driving in the system, respectively,

$$\ddot{\eta} + \omega^2 \eta = f(\eta, \dot{\eta}) + \xi \dot{\eta}, \tag{1}$$

$$f(\eta, \dot{\eta}) = \dot{q}_c - \alpha \dot{\eta} - q_a \sin(\omega_q t) \dot{\eta}, \tag{2}$$

$$q_c = \beta \eta - \kappa \frac{\eta^3}{3} + \gamma \frac{\eta^5}{5}. \tag{3}$$

Since the slow time scale oscillation (due to heat release or hydrodynamics) is coupled to the acoustic velocity fluctuation ($\dot{\eta}$), the noise associated must also change in correspondence with $\dot{\eta}$. Hence, we use a multiplicative white noise term as shown in Eq. (1).

ξ is white noise that follows the autocorrelation $\langle \xi \xi_\tau \rangle = \Gamma \delta(\tau)$, where Γ is the noise intensity. A sufficient amount of noise intensity is used to replicate the experimental dynamics. Prior to using multiplicative white noise, the model was tested without noise and with additive white noise. Without noise, the model showed bursting oscillations with equal interburst intervals. Further, even with additive white noise, interburst intervals are uniform. However, multiplicative noise [as shown in Eq. (1)] is able to replicate the nonuniform interburst intervals during bursting oscillations similar to Fig. 2(b). The system of equations is solved using the stochastic Runge-Kutta scheme with a step size of 10^{-4} s. The parametric values are: $\omega = 2\pi \times 320$ Hz, $\omega_q = 10$ Hz, $q_a = 20$ rad/s, $\beta = 50$ rad/s, $\kappa = 9$, $\gamma = 0.7$, and $\Gamma = 3.16$.

We capture the transition from stable operation to limit cycle oscillations with a gradual decrease in the damping coefficient (α) of the system keeping all other parameters fixed. Physically, the damping of a thermoacoustic system could decrease as a result of the different temperature profiles established in the combustor duct during the transition from stable operation to thermoacoustic instability. The time series of the acoustic pressure (η) along with their zoomed-in views obtained for different α are shown in Fig. 6. The temporal
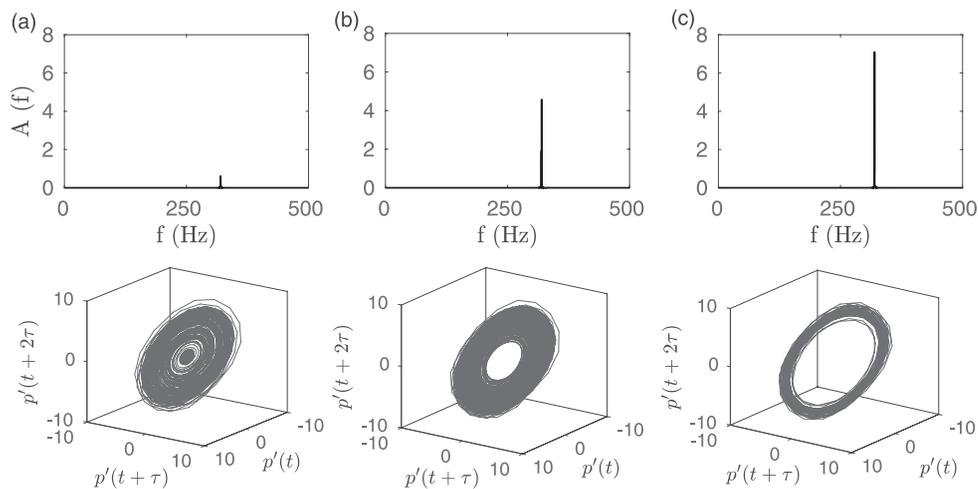
FIG. 7. The amplitude spectrum obtained through FFT and the reconstructed phase portrait during (a) bursting oscillations, (b) mixed mode oscillations, and (c) limit cycle oscillations.

evolution of η is shown from 6 s onwards, to discard any transient behavior due to numerical computations.

At $\alpha = 58$ rad/s [Fig. 6(a)], the model predicts a quiescent state. As we further decrease α [Fig. 6(b)], the oscillations resemble the combustor dynamics during bursting oscillations, wherein we observe dynamics alternating between quiescence and high amplitude oscillations in an apparently random manner with unequal interburst intervals. At $\alpha = 37$ rad/s [Fig. 6(c)], we obtain mixed mode oscillations with the dynamics switching between high amplitude and low amplitude periodic oscillations. Finally, for $\alpha = 5$ rad/s [Fig. 6(d)], we obtain limit cycle oscillations.

The amplitude spectra realized through FFT and the corresponding phase portraits plotted for a delay of $\tau = 4$ found by Cao's method[58] are shown in Figs. 7(a)–7(c) for bursting oscillations, mixed mode oscillations, and limit cycle oscillations, respectively. The amplitude spectrum during each dynamical state is similar to the one seen in the experimental data. The corresponding phase portraits also show the familiar disk-like structure without and with a hole during bursting oscillations [Fig. 7(a)] and mixed mode oscillations [Fig. 7(b)], respectively. Finally, we obtain a ring-like structure pertaining to limit cycle oscillations [Fig. 7(c)]. In summary, the model captures the essential features exhibited during the transition from stable operation to limit cycle oscillations in a thermoacoustic system.

IV. CONCLUSIONS

The dynamics of a multiple flame matrix burner is studied to characterize the route from stable operation to limit cycle oscillations, as we increase the equivalence ratio. In this study, we observed that the transition takes place through a novel route, compared to the already reported transition scenarios. We obtain bursting oscillations, characterized by alternating portions of high amplitude periodic oscillations followed by quiescent portions during the transition from stable operation to thermoacoustic instability. With further

increase in the equivalence ratio, we detect mixed mode oscillations featured by periodic oscillations switching between largely two amplitude levels. With further change in the control parameter, we obtain high amplitude limit cycle oscillations. The entire route is tracked using frequency evolution and phase portraits during each dynamical state. We observed that bursting oscillations and mixed mode oscillations display widely different amplitude levels across a range of frequencies. The bifurcation analysis highlighted the occurrence of high amplitude oscillations well before the onset of limit cycle oscillations. If observed in practical scenarios, this can have disastrous consequences leaving the combustor prone to structural failures. We conjecture that the nonlinear interaction between the slow temperature oscillations and the fast acoustic oscillations gives birth to bursting oscillations and mixed mode oscillations. Finally, a simple phenomenological model incorporating a slow time scale in addition to the fast acoustic time scale is constructed, which is successful in replicating the dynamical features observed in experiments.

REFERENCES

[1] T. C. Lieuwen, *Unsteady Combustor Physics* (Cambridge University Press, 2012).
[2] M. P. Juniper and R. Sujith, Annu. Rev. Fluid Mech. **50**, 661 (2018).
[3] J. W. S. Rayleigh, Nature **18**, 319 (1878).
[4] D. T. Harrje, "Liquid propellant rocket combustion instability," Technical Report NASA SP-194, 1972.

[5] J. C. Oefelein and V. Yang, J. Propul. Power **9**, 657 (1993).

[6] F. Culick and P. Kuentzmann, "Unsteady motions in combustion chambers for propulsion systems," Technical Report, NATO Research and Technology Organization Neuilly-Sur-Seine, France, 2006.

[7] V. Young, *Liquid Rocket Engine Combustion Instability* (AIAA, 1995), Vol. 169.

[8] E. Gopalakrishnan and R. Sujith, Int. J. Spray Combust. Dyn. **6**, 293 (2014).

[9] S. Etikyala and R. Sujith, Chaos **27**, 023106 (2017).

[10] P. Subramanian, S. Mariappan, R. Sujith, and P. Wahi, Int. J. Spray Combus. Dyn. **2**, 325 (2010).

[11] F. Weng, M. Zhu, and L. Jing, Int. J. Spray Combust. Dyn. **6**, 247 (2014).

[12] J. Tony, E. Gopalakrishnan, E. Sreelekha, and R. Sujith, Phys. Rev. E **92**, 062902 (2015).

[13] S. Mondal, V. R. Unni, and R. Sujith, J. Fluid Mech. **811**, 659 (2017).

[14] H. Gotoda, H. Nikimoto, T. Miyano, and S. Tachibana, Chaos **21**, 013124 (2011).

[15] V. Nair, G. Thampi, and R. Sujith, J. Fluid Mech. **756**, 470 (2014).

[16] H. Gotoda, Y. Shinoda, M. Kobayashi, Y. Okuno, and S. Tachibana, Phys. Rev. E **89**, 022910 (2014).

[17] S. Domen, H. Gotoda, T. Kuriyama, Y. Okuno, and S. Tachibana, Proc. Combust. Inst. **35**, 3245 (2015).

[18] M. Murugesan and R. I. Sujith, "Intermittency in combustion dynamics," in *51st AIAA/SAE/ASEE Joint Propulsion Conference* (AIAA, 2015), p. 3967.

[19] S. A. Pawar, R. Vishnu, M. Vadivukkarasan, M. Panchagnula, and R. Sujith, J. Eng. Gas Turbine Power **138**, 041505 (2016).

[20] D. Ebi, A. Denisov, G. Bonciolini, E. Boujo, and N. Noiray, J. Eng. Gas Turbine Power **140**, 061504 (2018).

[21] S. A. Pawar and R. I. Sujith, J. Combust. Soc. Jpn. **60**, 99 (2018).

[22] T. Selvakumaran and N. Kadiresh, Propellants Explos. Pyrotech. **43**, 251 (2018).

[23] V. Nair and R. Sujith, J. Fluid Mech. **747**, 635 (2014).

[24] V. R. Unni and R. I. Sujith, in *52nd AIAA/SAE/ASEE Joint Propulsion Conference* (AIAA, 2016), p. 4649.

[25] V. Unni, V. Nair, and R. Sujith, Provisional patent, filed (8 November 2013).

[26] S. A. Pawar, A. Seshadri, V. R. Unni, and R. Sujith, J. Fluid Mech. **827**, 664 (2017).

[27] V. Nair and R. Sujith, Combust. Sci. Technol. **187**, 1821 (2015).

[28] V. R. Unni and R. Sujith, Proc. Combust. Inst. **36**, 3791 (2017).

[29] L. Kabiraj, R. Sujith, and P. Wahi, J. Eng. Gas Turbine Power **134**, 031502 (2012).

[30] K. Kashinath, I. C. Waugh, and M. P. Juniper, J. Fluid Mech. **761**, 399 (2014).

[31] R. Vishnu, R. Sujith, and P. Aghalayam, Combust. Sci. Technol. **187**, 894 (2015).

[32] Y. Guan, P. Liu, B. Jin, V. Gupta, and L. K. Li, Exp. Thermal Fluid Sci. **98**, 217 (2018).

[33] V. R. Unni, Y. M. Prasaad, N. Ravi, S. M. Iqbal, B. Pesala, and R. Sujith, Int. J. Spray Combust. Dyn. **7**, 113 (2015).

[34] F. Joos and D. Vortmeyer, Combust. Flame **65**, 253 (1986).

[35] C. Kuehn, *Multiple Time Scale Dynamics* (Springer, 2015), Vol. 191.

[36] E. M. Izhikevich, SIAM Rev. **43**, 315 (2001).

[37] E. M. Izhikevich, *Dynamical Systems in Neuroscience* (MIT Press, 2007).

[38] J. Rinzel, in *Mathematical Topics in Population Biology, Morphogenesis and Neurosciences* (Springer, 1987), pp. 267–281.

[39] F. D'Alba and C. Lucarini, Bioelectrochem. Bioenerg. **38**, 185 (1995).

[40] C. Hammond, H. Bergman, and P. Brown, Trends Neurosci. **30**, 357 (2007).

[41] E. Knobloch and J. Moehlis, "Bursting mechanisms for hydrodynamical systems," in *Pattern Formation in Continuous and Coupled Systems* (Springer, New York, 1999), pp. 157–174.

[42] C. J. Lawn and G. Penelet, Int. J. Spray Combust. Dyn. **10**, 3 (2018).

[43] J. Wu, Q. Li, and F. Guo, J. Therm. Sci. **12**, 51 (2003).

[44] A. S. Abduljalil, Z. Yu, and A. J. Jaworski, Proc. Inst. Mech. Eng. Pt A J. Power Energy **226**, 822 (2012).

[45] M. Desroches, J. Guckenheimer, B. Krauskopf, C. Kuehn, H. M. Osinga, and M. Wechselberger, SIAM Rev. **54**, 211 (2012).

[46] M. A. Kramer, R. D. Traub, and N. J. Kopell, Phys. Rev. Lett. **101**, 068103 (2008).

[47] J. Hudson, M. Hart, and D. Marinko, J. Chem. Phys. **71**, 1601 (1979).

[48] V. Petrov, S. K. Scott, and K. Showalter, J. Chem. Phys. **97**, 6191 (1992).

[49] A. Roberts, E. Widiasih, M. Wechselberger, and C. K. Jones, Physica D Nonlinear Phenom. **292**, 70 (2015).

[50] M. Mikikian, M. Cavarroc, L. Couëdel, Y. Tessier, and L. Boufendi, Phys. Rev. Lett. **100**, 225005 (2008).

[51] V. R. Unni and R. Sujith, J. Fluid Mech. **784**, 30 (2015).

[52] E. Gopalakrishnan, Y. Sharma, T. John, P. S. Dutta, and R. Sujith, Sci. Rep. **6**, 35310 (2016).

[53] N. Noiray, J. Eng. Gas Turbine Power **139**, 041503 (2017).

[54] X. Han and Q. Bi, Commun. Nonlinear Sci. Numer. Simul. **16**, 4146 (2011).

[55] X. Han and Q. Bi, Nonlinear Dyn. **68**, 275 (2012).

[56] X. Han, Q. Bi, P. Ji, and J. Kurths, Phys. Rev. E **92**, 012911 (2015).

[57] C. Kuehn, Physica D Nonlinear Phenom. **240**, 1020 (2011).

[58] L. Cao, Physica D Nonlinear Phenom. **110**, 43 (1997).